A single high-zinc activation enhancer can control two genes oriented head-to-head in *C. elegans*

Hanwenheng Liu[1], Brian Earley[1,2], Adelita Mendoza[1,3], Patrick Hunt[1], Sean Teng[1,4], Daniel L. Schneider[1], Kerry Kornfeld[1,*]

[1] Department of Developmental Biology, Washington University School of Medicine, 660 S. Euclid Ave, St. Louis, MO 63130, USA

[2] Current address: Blackfoot High School, 870 S. Fisher Avenue, Blackfoot, Idaho 83221, USA

[3] Current address: University of Colorado at Boulder

[4] Current address: Center for Structural Biology, Center for Cancer Research, National Cancer Institute, Frederick, MD 21702-1201, USA

* Corresponding author. Email: kornfeld@wustl.edu

Running head:

One HZA enhancer controls two head-to-head genes

Keyword:

Zinc metabolism, high-zinc activation element, HZA, enhancer, divergent transcription, *C. elegans*

Abstract

Enhancers play critical roles in gene expression, but a full understanding of their complex functions has yet to be defined. The cellular response to excess zinc levels in *C. elegans* requires the HIZR-1 transcription factor, which binds the high-zinc activation (HZA) enhancer in the promoters of multiple target genes. Cadmium hijacks the excess zinc response by binding and activating HIZR-1. By analyzing the genome-wide transcriptional response to excess zinc and cadmium, we identified two positions in the genome where head-to-head oriented genes are both induced by metals. In both examples, a single predicted HZA enhancer is positioned between the two translational start sites. We hypothesized that a single enhancer can control both head-to-head genes, an arrangement that has not been extensively characterized. To test this hypothesis, we used CRISPR genome editing to precisely delete the HZA^{mT} enhancer positioned between *mtl-2* and *T08G5.1*, and the HZA^{cF} enhancer positioned between *cdr-1* and *F35E8.10*. In both examples, deleting the enhancer caused both head-to-head genes to lose metal-activated transcription, whereas the induction of more distant genes was not strongly affected. These studies rigorously document that a single HZA enhancer can control two head-to-head genes, advancing our understanding of the diverse functions of enhancers.

Article Summary

Enhancers are critical for gene expression, but a full understanding their functions has yet to be elucidated. We discovered two positions in the *C. elegans* genome where a pair of head-to-head oriented genes are both transcriptionally activated by the metals zinc and cadmium; in both cases, one high-zinc activation (HZA) enhancer is positioned between the translation start sites. When these HZA enhancers were deleted by genome engineering, both head-to-head genes lost metal-activated transcription. These results demonstrate that a single HZA enhancer can control two head-to-head genes, advancing the understanding of enhancer function.

43 **Introduction**

44 Zinc is essential, but excess zinc is toxic (Coleman 1992; Hambidge 2000; Sandstead 2015;
45 Zoroddu et al. 2019). Thus, animals evolved homeostatic mechanisms to maintain zinc in an
46 appropriate concentration range. In *C. elegans*, the HIZR-1 nuclear receptor transcription factor
47 is the master regulator of high zinc homeostasis. In excess zinc conditions, HIZR-1 directly binds
48 zinc, translocates to the nucleus, binds the HZA (High Zinc Activation) enhancer, and promotes
49 transcriptional activation (Roh et al. 2015; Dietrich et al. 2016; Warnhoff et al. 2017; Earley,
50 Mendoza, et al. 2021). Direct target genes have HZA enhancers, such as *cdf-2* and *ttm-1,* which
51 encode zinc transporters that reduce cytosolic zinc levels by sequestration in lysosome-related
52 organelles or excretion into the intestinal lumen, respectively (Davis et al. 2009; Roh et al. 2013;
53 Roh et al. 2015). Additional direct target genes include the metallothionines, *mtl-1* and *mtl-2*, and
54 *hizr-1* itself (Hall et al. 2012; Roh et al. 2012; Roh et al. 2015; Warnhoff et al. 2017; Mendoza et
55 al. 2024). Cadmium can directly bind HIZR-1, leading to the activation of genes that contain
56 HZA enhancers; thus, cadmium-responsive genes like *cdr-1* are also regulated by the HZA
57 element (Earley, Cubillas, et al. 2021).

58 Enhancers are *cis*-regulatory DNA sequences that either enhance or repress gene expression
59 (Banerji et al. 1981; Levine 2010). By recruiting various transcription factors, enhancers drive
60 cell differentiation and regulate stress response pathways (Panigrahi and O'Malley 2021).
61 Enhancers function at various locations relative to their target genes. They can be located either
62 up- or downstream of the target genes, as close as under 1kb or over 100kb away. A single
63 enhancer may regulate multiple genes (Chen et al. 2013; Mills et al. 2020). Usually, these genes
64 are encoded on the same DNA strand in a series, and the enhancer is positioned either 5' or 3' of
65 the series of genes, similar to operons in bacteria (Lercher et al. 2003; Cutter et al. 2009). When

66 two genes that are encoded on different DNA strands flank a common 5' region, they are called
67 head-to-head genes. Head-to-head genes are widespread in the *C. elegans* and human genomes;
68 in these cases, transcription of both genes is initiated from the common 5' region. This is called
69 "divergent transcription" (Adachi and Lieber 2002; Trinklein et al. 2004; Seila et al. 2009;
70 Ibrahim et al. 2018). The common 5' regions may contain enhancers that in principle could
71 regulate one or both transcripts. However, few examples of this situation have been analyzed in
72 detail. Examples of head-to-head gene pairs that have been analyzed in mice and chordates
73 indicate that enhancers in the common 5' region regulate one gene or the other, but not both,
74 which ensures cell type-specific gene expression (Swamynathan and Piatigorsky 2002; Hozumi
75 et al. 2013). Whether this logic also applies to the HZA enhancer in *C. elegans* is unknown.
76 The function of the HZA enhancer was previously analyzed using transgenic animals with
77 extrachromosomal arrays — in this context, the HZA enhancer was demonstrated to be necessary
78 for the zinc-induced activation of the *mtl-2* gene and sufficient to confer zinc-induced activation
79 on a *pes-10* basal promoter (Roh et al. 2015). However, the function of endogenous HZA
80 enhancers has not been reported. Here we used CRISPR genome editing to directly evaluate the
81 function of endogenous HZA enhancers. We examined two examples of head-to-head genes in
82 *C. elegans* that are both activated by cadmium (Earley, Cubillas, et al. 2021). Our results indicate
83 that a single HZA enhancer can control metal-activated transcription of both head-to-head
84 oriented genes. Thus, the regulatory function of a single HZA enhancer is divergent and acts on
85 two direct target genes, elucidating the functional capacity of this important DNA control
86 element.

87 **Results**

88 Identification of two genomic regions containing adjacent genes that are oriented head-to-head
89 and regulated by cadmium

90 Earley et al. (2021) identified many *C. elegans* genes that are activated by cadmium in
91 wild-type animals. By analyzing the chromosomal locations of these genes, we noticed that a
92 region of chromosome V (~14,018,911) contains two activated genes oriented head-to-head. One
93 gene is *mtl-2,* which encodes a *C. elegans* metallothionein protein that has been characterized
94 extensively for its roles in cadmium and zinc biology (Bofill et al. 2009; Zeitoun-Ghandour et al.
95 2010; Hall et al. 2012; Essig et al. 2024). The other gene is *T08G5.1,* which encodes an
96 uncharacterized protein. Roh et al. (2015) reported that the *mtl-2* promoter contains a predicted
97 HZA enhancer that promotes gene activation by zinc and cadmium. This HZA element, named
98 "HZA^{mT}" hereafter, is positioned between these two genes: the start codon ATGs of *mtl-2* and
99 *T08G5.1* are 277bp and 288bp from the HZA^{mT} element, respectively (Fig.1A). To quantify the
100 transcriptional response to cadmium, we exposed WT animals at the L4 stage to 100µM
101 cadmium for 16 hours, prepared RNA, and determined mRNA levels by quantitative reverse
102 transcriptase polymerase chain reaction (qRT-PCR) (Earley, Cubillas, et al. 2021). Compared to
103 control worms not exposed to cadmium, *mtl-2* and *T08G5.1* mRNA levels were significantly
104 increased by 5.4 log2 fold (~42x) and 7.6 log2 fold (~190x), respectively (Fig.1B-D).

105 We noticed another example of two genes oriented head-to-head that are both activated by
106 cadmium on chromosome V (~15,921,253). One gene is *cdr-1*, which was identified and named
107 after its strong induction by cadmium (Hall et al. 2012). The other gene is *F35E8.10,* which
108 encodes an uncharacterized protein. By searching the region between these two genes, Roh et al.
109 (2015) identified a predicted HZA element, named "HZA^{cF}" hereafter: the start codon ATGs of

110 *cdr-1* and *F35E8.10* are 108bp and 908bp from the HZA^{cF} element, respectively (Fig.1E).
111 Compared to control worms not exposed to cadmium, *cdr-1* and *F35E8.10* mRNA levels were
112 significantly increased by 8.1 log2 fold (~270x) and 3.3 log2 fold (~10x), respectively (Fig.1F-
113 G). For these two genes, the increase in mRNA levels correlated with the distance from the
114 predicted HZA element (Fig.1H).

115 <u>*hizr-1* was necessary for cadmium-mediated transcript accumulation of *mtl-2*, *T08G5.1, cdr-1,*</u>
116 <u>and *F35E8.10*</u>

117 Earley et al. (2021) demonstrated that cadmium hijacks the high zinc response by directly
118 binding and activating HIZR-1. To test the model that HIZR-1 is necessary for activation of
119 these four genes in response to cadmium, we used qPCR to quantify transcript levels in a strong
120 loss-of-function mutant, *hizr-1(am286* Q87STOP) (Warnhoff et al. 2017). Indeed, all four genes
121 were affected. *mtl-2*, *T08G5.1, F35E8.10,* and *cdr-1* mRNA levels were not significantly
122 different in *hizr-1* mutants treated with cadmium or untreated. In addition, transcript levels of
123 *mtl-2*, *T08G5.1,* and *cdr-1* were significantly lower in *hizr-1* mutants treated with cadmium
124 compared to wild-type animals treated with cadmium (Fig.1). *F35E8.10* transcript levels were
125 lower in *hizr-1* mutants treated with cadmium compared to wild-type animals treated with
126 cadmium, but this trend was not significant with this sample size (Fig.1F). Thus, *hizr-1* is
127 necessary for the cadmium induced transcript accumulation of these genes.

128 <u>A single HZA element mediates transcriptional activation of *mtl-2* and *T08G5.1* in response to</u>
129 <u>metals.</u>

130 Because HIZR-1 directly binds the HZA element, we hypothesized that the HZA elements
131 mediated transcript accumulation in response to metal. To evaluate this model, we used
132 CRISPR/Cas9 to generate the *syb4265* mutation, a 15-bp deletion that removes the HZA^{mT}

133 element (Fig.2B; labeled "HZA^{mT}Δ"). Because zinc is the physiological metal that activates
134 HIZR-1, we first examined the response to excess zinc. WT and *syb4265* animals at the L4 stage
135 were cultured on noble agar minimal media (NAMM) with either no additional metals (replete
136 zinc) or 200µM supplemental zinc (excess zinc) for 16 hours, and gene expression levels were
137 quantified by qPCR. Compared to control worms in zinc replete medium, WT animals in zinc
138 excess medium displayed *mtl-2* and *T08G5.1* mRNA levels that were significantly increased by
139 3.7 log2 fold (~13x) and 4.2 log2 fold (~18x), respectively (Fig.2B-C). By contrast, *mtl-2* and
140 *T08G5.1* mRNA levels were not significantly different in *syb4265* mutants cultured in zinc
141 replete or excess medium. In addition, transcript levels were significantly lower in *syb4265*
142 mutants treated with excess zinc compared to WT animals treated with excess zinc (Fig.2B-C).
143 To determine the specificity of the transcriptional response to the deleted HZA^{mT} enhancer,
144 we examined zinc-regulated genes at distant genomic positions. Similar to WT animals in excess
145 zinc, *syb4256* mutants in excess zinc displayed significantly higher transcript levels for *mtl-1*,
146 *cdf-2*, *hizr-1*, and *cdr-1* and significantly lower transcript levels for *zipt-2.3*, indicating that the
147 *syb4256* mutation specifically affects adjacent, but not distant, genes (Fig.2E-F, S1).
148 To evaluate the function of the HZA^{mT} enhancer in response to cadmium, we exposed WT
149 and *syb4256* mutant animals at the L4 stage to NAMM with 0 or 100µM cadmium for 16 hours
150 and determined mRNA levels by qPCR. In WT animals, both *mtl-2* and *T08G5.1* mRNA levels
151 were significantly increased by cadmium exposure (Fig.S2A-B). By contrast, *syb4256* mutant
152 animals displayed much less robust levels of gene activation that were marginally significant for
153 *mtl-2* and not significant for *T08G5.1.* However, similar effects were observed for control genes
154 positioned far from the mutation, suggesting this strain may have an altered response to cadmium
155 compared to wild type (Fig.S2C-F).

156 A single HZA element mediates transcriptional activation of *cdr-1* and *F35E8.10* in response to
157 metals.

158 We used CRISPR/Cas9 to delete the HZA element between *cdr-1* and *F35E8.10*; the
159 *syb4134* mutation is a 14-bp deletion that removes 13bp of the HZA^{cF} element (Fig.3A-B;
160 labeled as "$HZA^{cF}\Delta$"). To evaluate the response of these genes to zinc, we quantified gene
161 expression levels of the WT and *syb4134* animals as described above. Compared to WT animals
162 on zinc replete medium, WT animals in zinc excess displayed *cdr-1* mRNA levels that were
163 significantly increased by 7.5 log2 fold (~180x). *F35E8.10* mRNA levels were increased by 1.7
164 log2 fold (3.2x), but this trend was not significant with this samples size (Fig.3C-D). By contrast,
165 in *syb4134* mutants lacking the HZA^{cF} element, *cdr-1* and *F35E8.10* mRNA levels were not
166 significantly different when treated with excess zinc or untreated. In addition, *cdr-1* transcript
167 levels were significantly lower in *syb4134* mutants treated with excess zinc compared to
168 wild-type animals treated with excess zinc (Fig 3D). Thus, the HZA^{cF} element was necessary for
169 zinc-induced transcription of both genes.

170 To determine the specificity of the transcriptional response to the deleted HZA^{cF} enhancer,
171 we examined control genes at distant genomic positions. Similar to WT animals in excess zinc,
172 *syb4134* mutants in excess zinc displayed significantly higher transcript levels for *mtl-1*, *cdf-2*,
173 *hizr-1*, *mtl-2*, and *T08G5.1,* and significantly lower transcript levels for *zipt-2.3*, indicating the
174 *syb4134* mutation specifically affects adjacent genes (Fig.3E-F, S3).

175 To evaluate the effect of the deleted HZA^{cF} enhancer on the response to cadmium, we
176 analyzed WT and *syb4134* mutant animals as described above. In WT animals, both *cdr-1* and
177 *F35E8.10* mRNA levels were significantly increased by cadmium exposure (Fig.S4A-B). By
178 contrast, *syb4134* mutant animals displayed much less robust levels of gene activation that were

179 not significant. For control genes positioned far from the mutation, *mtl-1*, *mtl-2*, and *T08G5.1,*
180 transcriptional activation by cadmium was similar in WT and *syb4134* mutant animals,
181 indicating that the HZA mutation affects adjacent, but not distant, genes (Fig.S4C-E).

182 A deletion of *mtl-2* did not influence transcription of *T08G5.1*

183 Our results establish that *mtl-2* and *T08G5.1* are regulated by the same HZA enhancer. If
184 these two genes compete for access to the HZA^{mT} element, then removing one gene might
185 increase transcription of the other. To evaluate this model, we analyzed *mtl-2(gk125*), which
186 deletes a region from 208bp upstream of the *mtl-2* translation start codon (ATG) to 584bp
187 downstream of the *mtl-2* STOP codon and inserts one adenine (Fig.2A; labeled "*mtl-2Δ*" in
188 Fig.4) (Hall et al. 2012; The C. elegans Deletion Mutant Consortium 2012). No deletions of
189 *T08G5.1* currently exist. The deleted region includes the predicted TATA box (TATAAAAG)
190 positioned 47bp upstream of the *mtl-2* ATG. The HZA^{mT} element is not deleted. As expected,
191 *mtl-2* mRNA was not reliably detected in *mtl-2(gk125*) animals. We evaluated the response of
192 WT and *mtl-2(gk125)* to excess zinc using the aforementioned method. Compared to animals in
193 zinc replete medium, WT and *mtl-2(gk125*) animals in zinc excess displayed *T08G5.1* mRNA
194 levels that were significantly increased by 4.6 log2 fold (~24x) and 4.7 log2 fold (~26x),
195 respectively (Fig 4A). Thus, deletion of *mtl-2* did not affect the transcription of *T08G5.1*.

196 The *mtl-2(gk125)* deletion results in the ATG start codon of the neighboring gene *srh-308*
197 becoming 281bp away from the HZA^{mT} element (Fig 2A). To evaluate the possibility that the
198 HZA^{mT} enhancer now regulates the new adjacent gene, we examined transcription of *srh-308* as
199 described above. *srh-308* displayed high C_T cycles in WT, indicating a low baseline transcription
200 activity (Fig.S5E). *srh-308* was not significantly induced by excess zinc in WT or *mtl-2(gk125)*
201 mutants (Fig.4B). Thus, *srh-308* does not appear to be regulated by the HZA element in this

202 mutant. One possible explanation for this observation is that the transcription start site of *srh-308*
203 is deleted in *mtl-2Δ* (Fig.S6) (Gu et al. 2012; Chen et al. 2013; Kruesi et al. 2013; Saito et al.
204 2013).

205 **Discussion**

206 Based on the analysis of cadmium activated genes reported by Earley et al. (2021), we
207 identified two examples of adjacent genes that are oriented head-to-head and both activated by
208 cadmium. In both examples, a predicted HZA enhancer is positioned between the two genes. To
209 address fundamental questions about the function of these HZA enhancers, we used CRISPR
210 genome engineering to create small deletions that remove these enhancers from the genome.
211 While genome editing technology has been used to study *cis*-regulatory elements in many
212 organisms, including enhancers in *C. elegans*, mice, and mammalian cells, it has not previously
213 been used to analyze the HZA enhancer (Moorthy and Mitchell 2016; Li et al. 2020; Froehlich et
214 al. 2021). Deleting the HZA^{mT} enhancer strongly reduced activation of both *mtl-2* and *T08G5.1*
215 in response to excess zinc and cadmium. Similarly, deleting the HZA^{cF} enhancer strongly
216 reduced activation of both *F35E8.10* and *cdr-1* in response to excess zinc and cadmium. These
217 results lead to several conclusions: (1) a single HZA enhancer can regulate two genes oriented
218 head-to-head, (2) by extension, these enhancers can function in either orientation. Orientation
219 independence is considered to be a hallmark of enhancers (Banerji et al. 1981); (3) these
220 enhancers can function at a variable distance; however, the strength of induction is correlated
221 with distance from the ATG start codon. The *F35E8.10* start codon is 908bp from the HZA^{cF}
222 enhancer, and the gene is weakly induced; the *mtl-2* and *T08G5.1* start codons are about 280bp
223 from the HZA^{mT} enhancer, and these genes are induced at an intermediate level; the *cdr-1* start
224 codon is 108bp from the HZA^{cF} enhancer, and the gene is strongly induced (Fig.1D, H; Fig.S5C-
225 D). Our analysis using genome engineering to delete endogenous HZA enhancers supports and
226 extends previous studies of HZA enhancers performed with extrachromosomal arrays (Roh et al.
227 2015; Earley, Cubillas, et al. 2021).

228 Enhancers were characterized as orientation-independent when studied on a vector (Banerji
229 et al. 1981). However, little is understood about the ability of a single enhancer to control two
230 genes oriented head-to-head. One factor that affects enhancer function is cell type. If the two
231 head-to-head genes are expressed in different cell types, then the enhancer might exhibit
232 different cell type-specific functions. Indeed, two groups reported orientation-dependent
233 enhancer functions in mice and chordate *Ciona intestinalis* in different cell types (Swamynathan
234 and Piatigorsky 2002; Hozumi et al. 2013). This cell type-specificity may be controlled by other
235 nearby enhancer elements. In *C. elegans*, the HZA element is often in close proximity to a
236 GATA element, an intestine-specific enhancer (Roh et al. 2015). At the *mtl-2*/*T08G5.1* locus,
237 there are two predicted GATA elements flanking the HZA element (Moilanen et al. 1999; Roh et
238 al. 2015). Another factor that affects enhancer function is chromatin regulators, such as
239 insulators that block access of RNA polymerase II to one flanking gene (Luan et al. 2022;
240 Hamamoto et al. 2023). A lack of CTCF homologs in *C. elegans* may explain the ability of the
241 HZA enhancer to function on both head-to-head genes (Heger et al. 2009).
242 How does a single enhancer control two genes? A widely supported model for enhancer
243 function is looping: proteins recruited to the enhancer and the promoter bring the two into a
244 dynamic enhancer-promoter contact (EPC) (Panigrahi and O'Malley 2021). The dynamic EPC
245 might be the rate-limiting factor in transcriptional activation of a target gene (Panigrahi et al.
246 2018). Thus, one possibility is that the HZA enhancer loops to one flanking gene at a time,
247 forming only one EPC; in this scenario, the two gene promoters might compete for access to the
248 EPC. To test this model, we deleted the *mtl-2* gene and examined transcription of *T08G5.1.*
249 Interestingly, transcription of *T08G5.1* was similar in the deletion mutant, indicating that the
250 EPC may not alternate between the two promoters. Perhaps the EPC interacts with the promoters

251 of both genes at the same time. MDT-15, a mediator subunit, is a co-activator for HIZR-1, and
252 may contribute to EPC formation (Shomer et al. 2019).

253 There are several possible reasons why this orientation of enhancers and promoters may
254 have evolved: 1) It is beneficial to have co-expression of two functionally related genes in
255 response to metal stress. If two head-to-head genes both function in the same pathway, a single
256 enhancer might be an efficient mechanism for mounting a response. 2) The "Sheltered Island
257 Hypothesis" speculates that functionally unrelated genes remain clustered or nested together
258 because any changes would be toxic to the essential genes in the cluster (Chen and Stein 2006).
259 3) One of the head-to-head genes may be a bystander gene that is neither beneficial nor toxic. If
260 co-regulation of these genes is not deleterious, then this arrangement may have evolved.
261 Whereas the *mtl-2* gene has been characterized extensively for a function in cadmium resistance,
262 the function of the *T08G5.1* gene has not been characterized (Almutairi et al. 2024). In a similar
263 manner, the *cdr-1* gene has been characterized for a function in cadmium resistance, but the
264 function of the *F35E8.10* gene has not been characterized. Thus, all three models are possible
265 explanations for this arrangement of genes.

266 **Methods**

267 Worm Handling and Culture

268 Animals were cultured on nematode growth media (NGM) dishes seeded with *E. coli* OP50
269 at 20°C (Brenner 1974) unless otherwise noted. We picked three L1-stage larvae onto fresh
270 NGM dishes weekly to maintain strains.

271 To minimize precipitation of metals during supplementation experiments, we cultured
272 animals on noble agar minimal media (NAMM) dishes (Warnhoff et al. 2017; Earley, Cubillas,
273 et al. 2021). Each NAMM dish contains 0.1% cholesterol and 3.7% noble agar. Zinc replete
274 NAMM has no supplemental metal. Zinc excess NAMM contains 200µM $ZnSO_4$. Cadmium
275 NAMM contains 100µM $CdCl_2$.

276 Strain generation

277 We used Bristol isolate N2 as wild type (Brenner 1974). The *hizr-1(am286)* strain, WU1958,
278 was generated by outcrossing the parental strain, WU1500, to N2 three times. The *am286* allele
279 contains a C259T mutation that changes Q87 to STOP (Warnhoff et al. 2017).

280 We worked with SunyBiotech (www.sunybiotech.com) to generate CRISPR knockout
281 strains, PHX4134 and PHX4265. PHX4134 contains *syb4134*, a 15bp deletion that precisely
282 removes 13bp of the HZA^{cF} element (AAA CAG AAA CTA CA) that is positioned 108bp
283 upstream of the *cdr-1* translation start site (ATG) (Fig.3). PHX4265 contains *syb4265*, a 15bp
284 deletion that removes the entire 15bp HZA^{mT} element (TAT CAC AAA CTA GAG) that is
285 positioned 278bp upstream of the *mtl-2* translation start site (ATG) (Fig.2). The deletions were
286 validated by Sanger DNA sequencing.

287 To analyze the *mtl-2(gk125)* mutation, we outcrossed VC128 five times to N2 to obtain the
288 strain WU946 (The C. elegans Deletion Mutant Consortium 2012). The *gk125* insertion/deletion

289 removes the region from 208bp upstream of *mtl-2* ATG to 584bp downstream of *mtl-2* STOP
290 codon (TAA) and inserts a single adenine (Fig.2). The insertion/deletion was validated by Sanger
291 DNA sequencing. DNA sequencing was performed using GENEWIZ (Azenta Life Sciences,
292 www.genewiz.com). See Table S2 for oligonucleotide primers.
293

294 **Data Availability**

295 All strains and primers are available upon request. Supplementary File 1 contains all qPCR data
296 processing spreadsheet (eg. Organized Data Cd, *hizr-1 am286*, Zn, etc), GraphPad Prism sheets,
297 and log2 average calculation sheets (for superplot). Corresponding folders to figures: "*hizr-1*
298 *am286*" – Fig 1, "Zn" – Fig 2 & 3, Sup Fig S1, S3, & S5, "Cd" – Sup Fig S2, S4, & S5, "*mtl-2*",
299 "*srh-308*" – Fig 4. Supplementary File 2 contains sequencing files for HZA^{mT} and HZA^{cF} loci.
300 "*cdr-1*_sequencing.seq" and "*mtl-2*_sequencing.seq" are Sanger sequencing results for the
301 knockout strains. "*mtl-2 gk125*" folder contains Sanger sequencing results for *gk125* allele
302 verification. Supplementary File 3 contains sequences of *mtl-2* homologs from *C. breneri*, *C.*
303 *briggsae*, and *C. remanei* used for alignment in Fig. 2. Files are made available online at
304 https://zenodo.org/records/13948425, DOI: 10.5281/zenodo.13948425.
305

306 **Acknowledgement**

307 We thank Barak Cohen and Mike Nonet for helpful discussions and the *Caenorhabditis* Genetics
308 Center and SUNY Biotech for providing strains. Brian Egan, Dana Shaw, and Vishnu
309 Saraswathy provided advice and assistance with qPCR procedures and data analysis.
310

311 **Funding**

Funding was provided by the NIH (grant R01 GM068598 received by K.K. and grant F31 ES030622 received by B.E.).

Conflicts of Interest

The authors declare no conflicts of interest.

317 **References**

318 Adachi N, Lieber MR. 2002. Bidirectional Gene Organization. Cell. 109(7):807–809.
319 doi:10.1016/S0092-8674(02)00758-4.

320 Almutairi N, Khan N, Harrison-Smith A, Arlt VM, Stürzenbaum SR. 2024. Stage-specific
321 exposure of *Caenorhabditis elegans* to cadmium identifies unique transcriptomic response
322 cascades and an uncharacterised cadmium responsive transcript. Metallomics.:mfae016.
323 doi:10.1093/mtomcs/mfae016.

324 Banerji J, Rusconi S, Schaffner W. 1981. Expression of a β-globin gene is enhanced by remote
325 SV40 DNA sequences. Cell. 27(2):299–308. doi:10.1016/0092-8674(81)90413-X.

326 Bofill R, Orihuela R, Romagosa M, Domènech J, Atrian S, Capdevila M. 2009. *Caenorhabditis*
327 *elegans* metallothionein isoform specificity – metal binding abilities and the role of histidine in
328 CeMT1 and CeMT2. The FEBS Journal. 276(23):7040–7056. doi:10.1111/j.1742-
329 4658.2009.07417.x.

330 Brenner S. 1974. The genetics of Caenorhabditis elegans. Genetics. 77(1):71–94.
331 doi:10.1093/genetics/77.1.71.

332 Chen N, Stein LD. 2006. Conservation and functional significance of gene topology in the
333 genome of Caenorhabditis elegans. Genome Res. 16(5):606–617. doi:10.1101/gr.4515306.

334 Chen RA-J, Down TA, Stempor P, Chen QB, Egelhofer TA, Hillier LW, Jeffers TE, Ahringer J.
335 2013. The landscape of RNA polymerase II transcription initiation in *C. elegans* reveals
336 promoter and enhancer architectures. Genome Res. 23(8):1339–1347.
337 doi:10.1101/gr.153668.112.

338 Coleman JE. 1992. ZINC PROTEINS: Enzymes, Storage Proteins, Transcription Factors, and
339 Replication Proteins. Annu Rev Biochem. 61(1):897–946.
340 doi:10.1146/annurev.bi.61.070192.004341.

341 Cutter AD, Dey A, Murray RL. 2009. Evolution of the Caenorhabditis elegans Genome.
342 Molecular Biology and Evolution. 26(6):1199–1234. doi:10.1093/molbev/msp048.

343 Davis DE, Roh HC, Deshmukh K, Bruinsma JJ, Schneider DL, Guthrie J, Robertson JD,
344 Kornfeld K. 2009. The Cation Diffusion Facilitator Gene *cdf-2* Mediates Zinc Metabolism in
345 *Caenorhabditis elegans*. Genetics. 182(4):1015–1033. doi:10.1534/genetics.109.103614.

346 Dietrich N, Tan C-H, Cubillas C, Earley BJ, Kornfeld K. 2016. Insights into zinc and cadmium
347 biology in the nematode Caenorhabditis elegans. Archives of Biochemistry and Biophysics.
348 611:120–133. doi:10.1016/j.abb.2016.05.021.

349 Earley BJ, Cubillas C, Warnhoff K, Ahmad R, Alcantar A, Lyon MD, Schneider DL, Kornfeld
350 K. 2021. Cadmium hijacks the high zinc response by binding and activating the HIZR-1 nuclear
351 receptor. Proc Natl Acad Sci USA. 118(42):e2022649118. doi:10.1073/pnas.2022649118.

352 Earley BJ, Mendoza AD, Tan C-H, Kornfeld K. 2021. Zinc homeostasis and signaling in the
353 roundworm C. elegans. Biochimica et Biophysica Acta (BBA) - Molecular Cell Research.
354 1868(1):118882. doi:10.1016/j.bbamcr.2020.118882.

355 Essig YJ, Leszczyszyn OI, Almutairi N, Harrison-Smith A, Blease A, Zeitoun-Ghandour S,
356 Webb SM, Blindauer CA, Stürzenbaum SR. 2024. Juggling cadmium detoxification and zinc
357 homeostasis: A division of labour between the two C. elegans metallothioneins. Chemosphere.
358 350:141021. doi:10.1016/j.chemosphere.2023.141021.

359 Froehlich JJ, Uyar B, Herzog M, Theil K, Glažar P, Akalin A, Rajewsky N. 2021. Parallel
360 genetics of regulatory sequences using scalable genome editing in vivo. Cell Reports.
361 35(2):108988. doi:10.1016/j.celrep.2021.108988.

362 Gu W, Lee H-C, Chaves D, Youngman EM, Pazour GJ, Conte D, Mello CC. 2012. CapSeq and
363 CIP-TAP Identify Pol II Start Sites and Reveal Capped Small RNAs as C. elegans piRNA
364 Precursors. Cell. 151(7):1488–1500. doi:10.1016/j.cell.2012.11.023.

365 Hall J, Haas KL, Freedman JH. 2012. Role of MTL-1, MTL-2, and CDR-1 in Mediating
366 Cadmium Sensitivity in Caenorhabditis elegans. Toxicological Sciences. 128(2):418–426.
367 doi:10.1093/toxsci/kfs166.

368 Hamamoto K, Umemura Y, Makino S, Fukaya T. 2023. Dynamic interplay between non-coding
369 enhancer transcription and gene activity in development. Nat Commun. 14(1):826.
370 doi:10.1038/s41467-023-36485-1.

371 Hambidge M. 2000. Human Zinc Deficiency. The Journal of Nutrition. 130(5):1344S-1349S.
372 doi:10.1093/jn/130.5.1344S.

373 Heger P, Marin B, Schierenberg E. 2009. Loss of the insulator protein CTCF during nematode
374 evolution. BMC Mol Biol. 10(1):84. doi:10.1186/1471-2199-10-84.

375 Hozumi A, Yoshida R, Horie T, Sakuma T, Yamamoto T, Sasakura Y. 2013. Enhancer activity
376 sensitive to the orientation of the gene it regulates in the chordate genome. Developmental
377 Biology. 375(1):79–91. doi:10.1016/j.ydbio.2012.12.012.

378 Ibrahim MM, Karabacak A, Glahs A, Kolundzic E, Hirsekorn A, Carda A, Tursun B, Zinzen RP,
379 Lacadie SA, Ohler U. 2018. Determinants of promoter and enhancer transcription directionality
380 in metazoans. Nat Commun. 9(1):4472. doi:10.1038/s41467-018-06962-z.

381 Kruesi WS, Core LJ, Waters CT, Lis JT, Meyer BJ. 2013. Condensin controls recruitment of
382 RNA polymerase II to achieve nematode X-chromosome dosage compensation. Elife. 2:e00808.
383 doi:10.7554/eLife.00808.

384 Lercher MJ, Blumenthal T, Hurst LD. 2003. Coexpression of Neighboring Genes in
385 *Caenorhabditis Elegans* Is Mostly Due to Operons and Duplicate Genes. Genome Res.
386 13(2):238–243. doi:10.1101/gr.553803.

387 Levine M. 2010. Transcriptional Enhancers in Animal Development and Evolution. Current

388 Biology. 20(17):R754–R763. doi:10.1016/j.cub.2010.06.070.

389 Li K, Liu Y, Cao H, Zhang Y, Gu Z, Liu X, Yu A, Kaphle P, Dickerson KE, Ni M, et al. 2020.
390 Interrogation of enhancer function by enhancer-targeting CRISPR epigenetic editing. Nat
391 Commun. 11(1):485. doi:10.1038/s41467-020-14362-5.

392 Luan J, Vermunt MW, Syrett CM, Coté A, Tome JM, Zhang H, Huang A, Luppino JM, Keller
393 CA, Giardine BM, et al. 2022. CTCF blocks antisense transcription initiation at divergent
394 promoters. Nat Struct Mol Biol. 29(11):1136–1144. doi:10.1038/s41594-022-00855-y.

395 Mendoza AD, Dietrich N, Tan C-H, Herrera D, Kasiah J, Payne Z, Cubillas C, Schneider DL,
396 Kornfeld K. 2024. Lysosome-related organelles contain an expansion compartment that mediates
397 delivery of zinc transporters to promote homeostasis. Proc Natl Acad Sci USA.
398 121(7):e2307143121. doi:10.1073/pnas.2307143121.

399 Mills C, Muruganujan A, Ebert D, Marconett CN, Lewinger JP, Thomas PD, Mi H. 2020.
400 PEREGRINE: A genome-wide prediction of enhancer to gene relationships supported by
401 experimental evidence. Prokunina-Olsson L, editor. PLoS ONE. 15(12):e0243791.
402 doi:10.1371/journal.pone.0243791.

403 Moilanen LH, Fukushige T, Freedman JH. 1999. Regulation of Metallothionein Gene
404 Transcription. Journal of Biological Chemistry. 274(42):29655–29665.
405 doi:10.1074/jbc.274.42.29655.

406 Moorthy SD, Mitchell JA. 2016. Generating CRISPR/Cas9 Mediated Monoallelic Deletions to
407 Study Enhancer Function in Mouse Embryonic Stem Cells. JoVE.(110):53552.
408 doi:10.3791/53552.

409 Panigrahi A, O'Malley BW. 2021. Mechanisms of enhancer action: the known and the unknown.
410 Genome Biol. 22(1):108. doi:10.1186/s13059-021-02322-1.

411 Panigrahi AK, Foulds CE, Lanz RB, Hamilton RA, Yi P, Lonard DM, Tsai M-J, Tsai SY,
412 O'Malley BW. 2018. SRC-3 Coactivator Governs Dynamic Estrogen-Induced Chromatin
413 Looping Interactions during Transcription. Molecular Cell. 70(4):679-694.e7.
414 doi:10.1016/j.molcel.2018.04.014.

415 Roh HC, Collier S, Deshmukh K, Guthrie J, Robertson JD, Kornfeld K. 2013. ttm-1 Encodes
416 CDF Transporters That Excrete Zinc from Intestinal Cells of C. elegans and Act in a Parallel
417 Negative Feedback Circuit That Promotes Homeostasis. Eide DJ, editor. PLoS Genet.
418 9(5):e1003522. doi:10.1371/journal.pgen.1003522.

419 Roh HC, Collier S, Guthrie J, Robertson JD, Kornfeld K. 2012. Lysosome-Related Organelles in
420 Intestinal Cells Are a Zinc Storage Site in C. elegans. Cell Metabolism. 15(1):88–99.
421 doi:10.1016/j.cmet.2011.12.003.

422 Roh HC, Dimitrov I, Deshmukh K, Zhao G, Warnhoff K, Cabrera D, Tsai W, Kornfeld K. 2015.
423 A modular system of DNA enhancer elements mediates tissue-specific activation of transcription
424 by high dietary zinc in C. elegans. Nucleic Acids Research. 43(2):803–816.

425 doi:10.1093/nar/gku1360.

426 Saito TL, Hashimoto S, Gu SG, Morton JJ, Stadler M, Blumenthal T, Fire A, Morishita S. 2013.
427 The transcription start site landscape of *C. elegans*. Genome Res. 23(8):1348–1361.
428 doi:10.1101/gr.151571.112.

429 Sandstead HH. 2015. Zinc. In: Handbook on the Toxicology of Metals. Elsevier. p. 1369–1385.
430 [accessed 2024 Feb 6]. https://linkinghub.elsevier.com/retrieve/pii/B9780444594532000615.

431 Seila AC, Core LJ, Lis JT, Sharp PA. 2009. Divergent transcription: A new feature of active
432 promoters. Cell Cycle. 8(16):2557–2564. doi:10.4161/cc.8.16.9305.

433 Shomer N, Kadhim AZ, Grants JM, Cheng X, Alhusari D, Bhanshali F, Poon AF-Y, Lee MYY,
434 Muhuri A, Park JI, et al. 2019. Mediator subunit MDT-15/MED15 and Nuclear Receptor HIZR-
435 1/HNF4 cooperate to regulate toxic metal stress responses in Caenorhabditis elegans. Blackwell
436 TK, editor. PLoS Genet. 15(12):e1008508. doi:10.1371/journal.pgen.1008508.

437 Swamynathan SK, Piatigorsky J. 2002. Orientation-dependent Influence of an Intergenic
438 Enhancer on the Promoter Activity of the Divergently Transcribed Mouse Shsp/αB-crystallin
439 andMkbp/HspB2 Genes. Journal of Biological Chemistry. 277(51):49700–49706.
440 doi:10.1074/jbc.M209700200.

441 The C. elegans Deletion Mutant Consortium. 2012. Large-Scale Screening for Targeted
442 Knockouts in the *Caenorhabditis elegans* Genome. G3 Genes|Genomes|Genetics. 2(11):1415–
443 1425. doi:10.1534/g3.112.003830.

444 Trinklein ND, Aldred SF, Hartman SJ, Schroeder DI, Otillar RP, Myers RM. 2004. An
445 Abundance of Bidirectional Promoters in the Human Genome. Genome Res. 14(1):62–66.
446 doi:10.1101/gr.1982804.

447 Warnhoff K, Roh HC, Kocsisova Z, Tan C-H, Morrison A, Croswell D, Schneider DL, Kornfeld
448 K. 2017. The Nuclear Receptor HIZR-1 Uses Zinc as a Ligand to Mediate Homeostasis in
449 Response to High Zinc. Sengupta P, Tissenbaum H, editors. PLoS Biol. 15(1):e2000094.
450 doi:10.1371/journal.pbio.2000094.

451 Zeitoun-Ghandour S, Charnock JM, Hodson ME, Leszczyszyn OI, Blindauer CA, Stürzenbaum
452 SR. 2010. The two *Caenorhabditis elegans* metallothioneins (CeMT-1 and CeMT-2)
453 discriminate between essential zinc and toxic cadmium. The FEBS Journal. 277(11):2531–2542.
454 doi:10.1111/j.1742-4658.2010.07667.x.

455 Zoroddu MA, Aaseth J, Crisponi G, Medici S, Peana M, Nurchi VM. 2019. The essential metals
456 for humans: a brief overview. Journal of Inorganic Biochemistry. 195:120–129.
457 doi:10.1016/j.jinorgbio.2019.03.013.

Fig 1

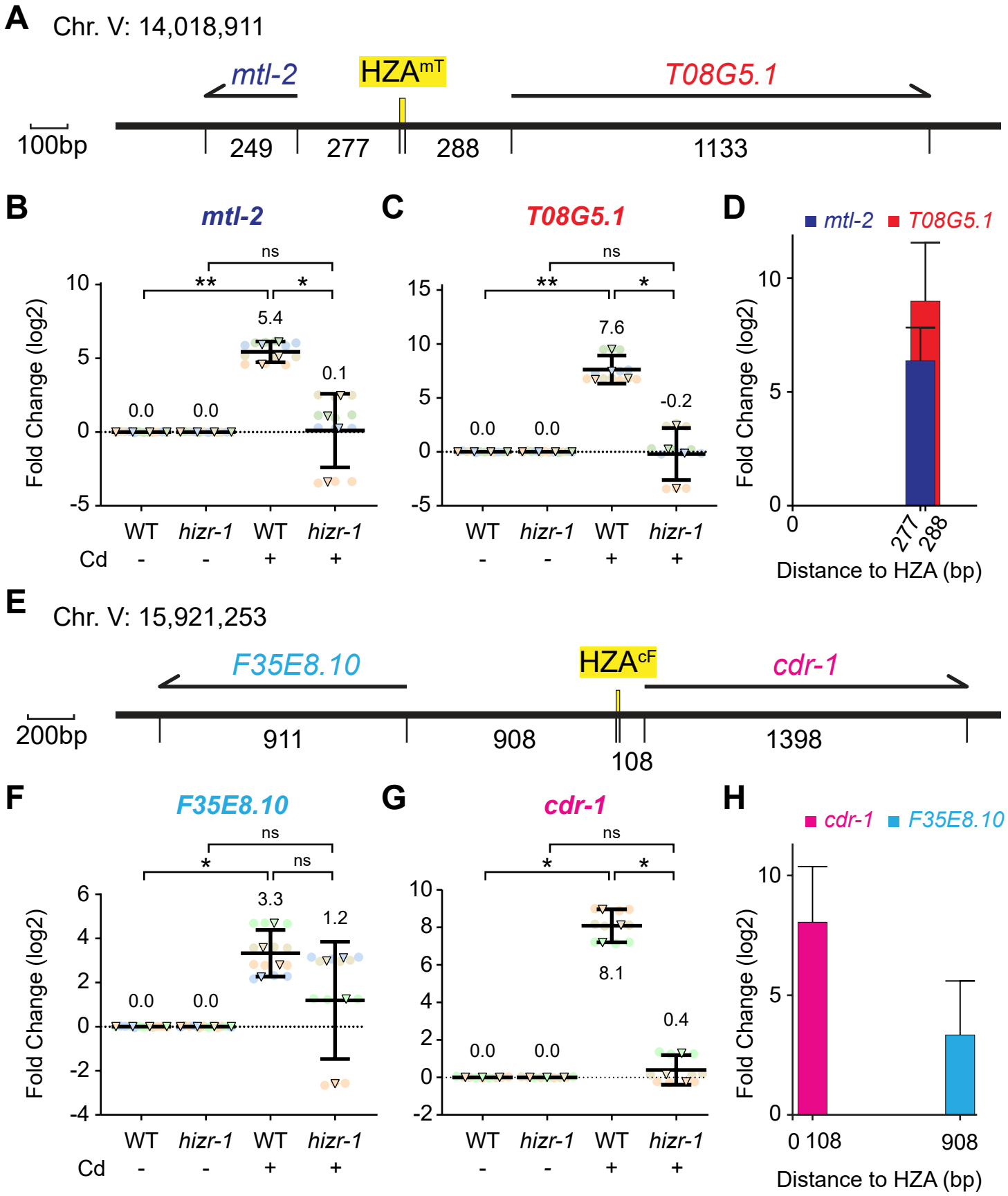
A
Chr. V: 14,018,911
mtl-2
HZAmT
T08G5.1
100bp
249
277
288
1133
B
mtl-2
C
T08G5.1
D
mtl-2
T08G5.1
Fold Change (log2)
ns
**
*
5.4
0.1
0.0
0.0
7.6
-0.2
WT
hizr-1
Cd
Distance to HZA (bp)
E
Chr. V: 15,921,253
F35E8.10
HZAcF
cdr-1
200bp
911
908
108
1398
F
F35E8.10
G
cdr-1
H
cdr-1
F35E8.10
3.3
1.2
8.1
0.4

Fig 2

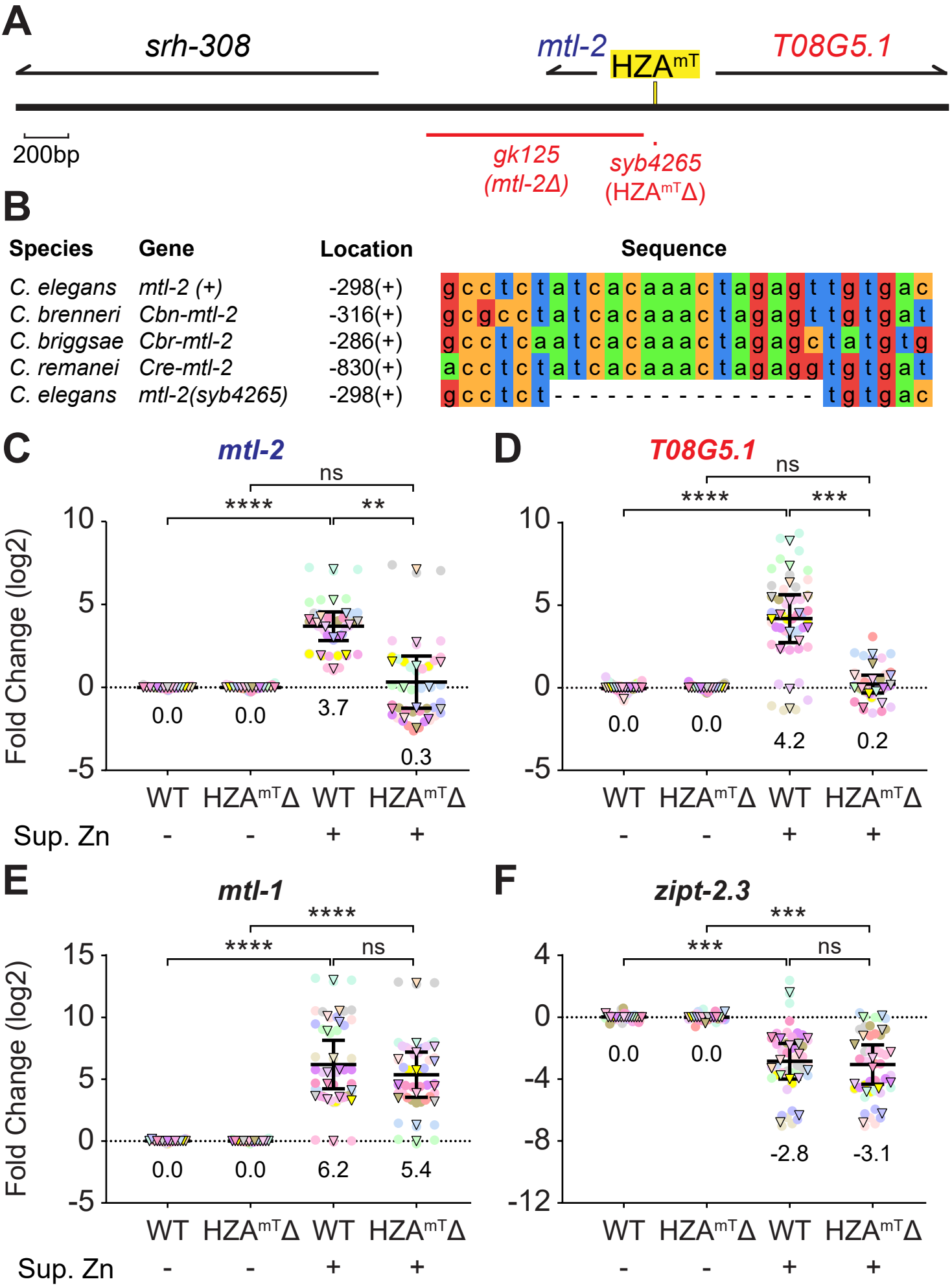
A
srh-308
mtl-2
HZAmT
T08G5.1
200bp
gk125
(mtl-2Δ)
syb4265
(HZAmTΔ)
B
Species
Gene
Location
Sequence
C. elegans mtl-2 (+) -298(+) gcctctatcacaaactagagttgtgac
C. brenneri Cbn-mtl-2 -316(+) gcgcctatcacaaactagagttgtgat
C. briggsae Cbr-mtl-2 -286(+) gcctcaatcacaaactagagctatgtg
C. remanei Cre-mtl-2 -830(+) acctctatcacaaactagaggtgtgat
C. elegans mtl-2(syb4265) -298(+) gcctct----------tgtgac
C
mtl-2
Fold Change (log2)
ns
****
**
0.0
0.0
3.7
0.3
WT
HZAmTΔ
WT
HZAmTΔ
Sup. Zn
-
-
+
+
D
T08G5.1
ns
****
***
0.0
0.0
4.2
0.2
E
mtl-1
****
****
ns
0.0
0.0
6.2
5.4
F
zipt-2.3
***
***
ns
0.0
0.0
-2.8
-3.1

Fig 3

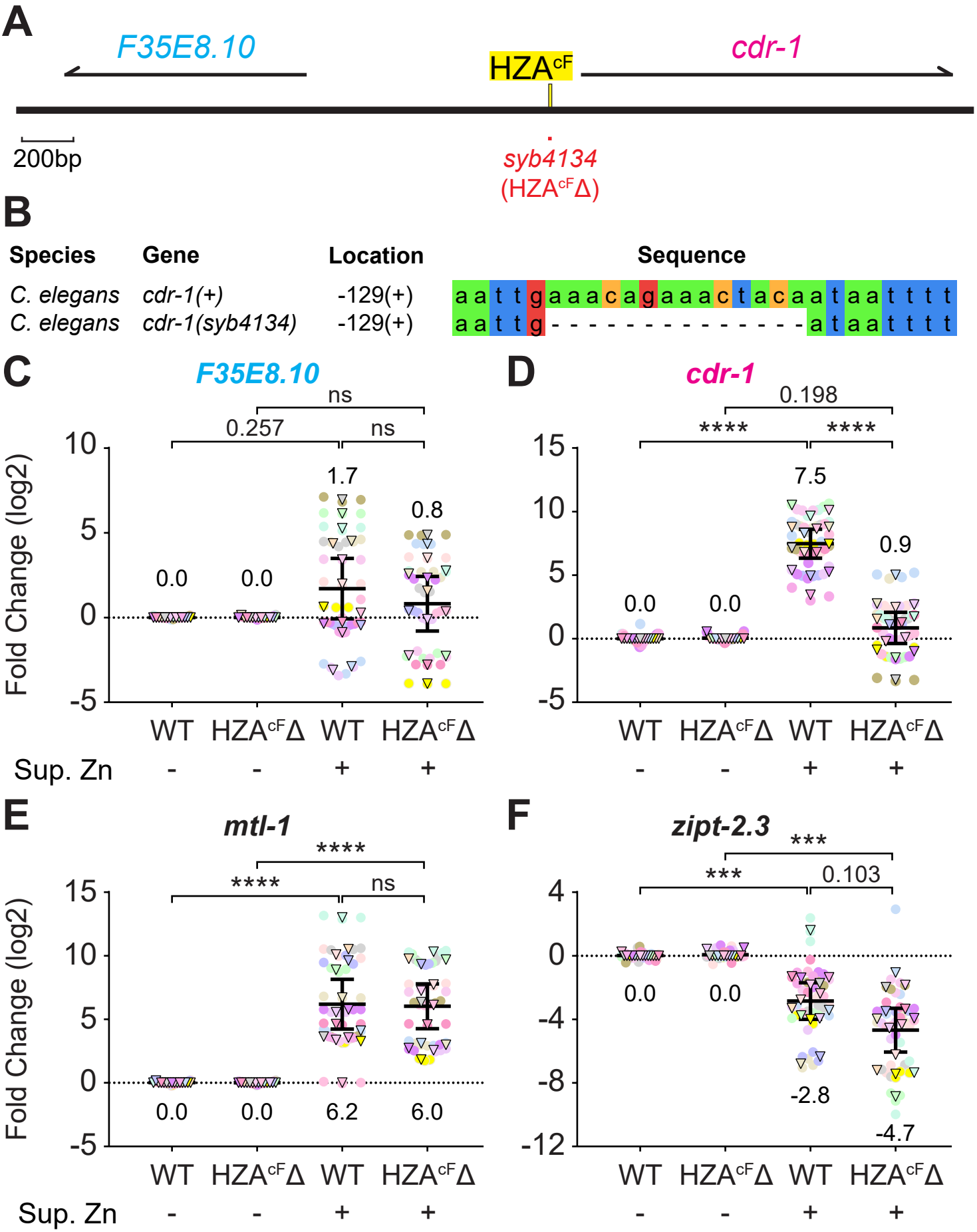
A
F35E8.10
HZA^cF
cdr-1
200bp
syb4134
(HZA^cFΔ)
B
Species
Gene
Location
Sequence
C. elegans
cdr-1(+)
-129(+)
aattgaaacagaaactacaataattttt
C. elegans
cdr-1(syb4134)
-129(+)
aattg----------ataattttt
C
F35E8.10
Fold Change (log2)
ns
0.257
ns
1.7
0.8
0.0
0.0
WT
HZA^cFΔ
WT
HZA^cFΔ
Sup. Zn
-
-
+
+
D
cdr-1
0.198
****
****
7.5
0.9
0.0
0.0
E
mtl-1
****
****
ns
6.2
6.0
0.0
0.0
F
zipt-2.3
***
***
0.103
-2.8
-4.7
0.0
0.0

Fig 4

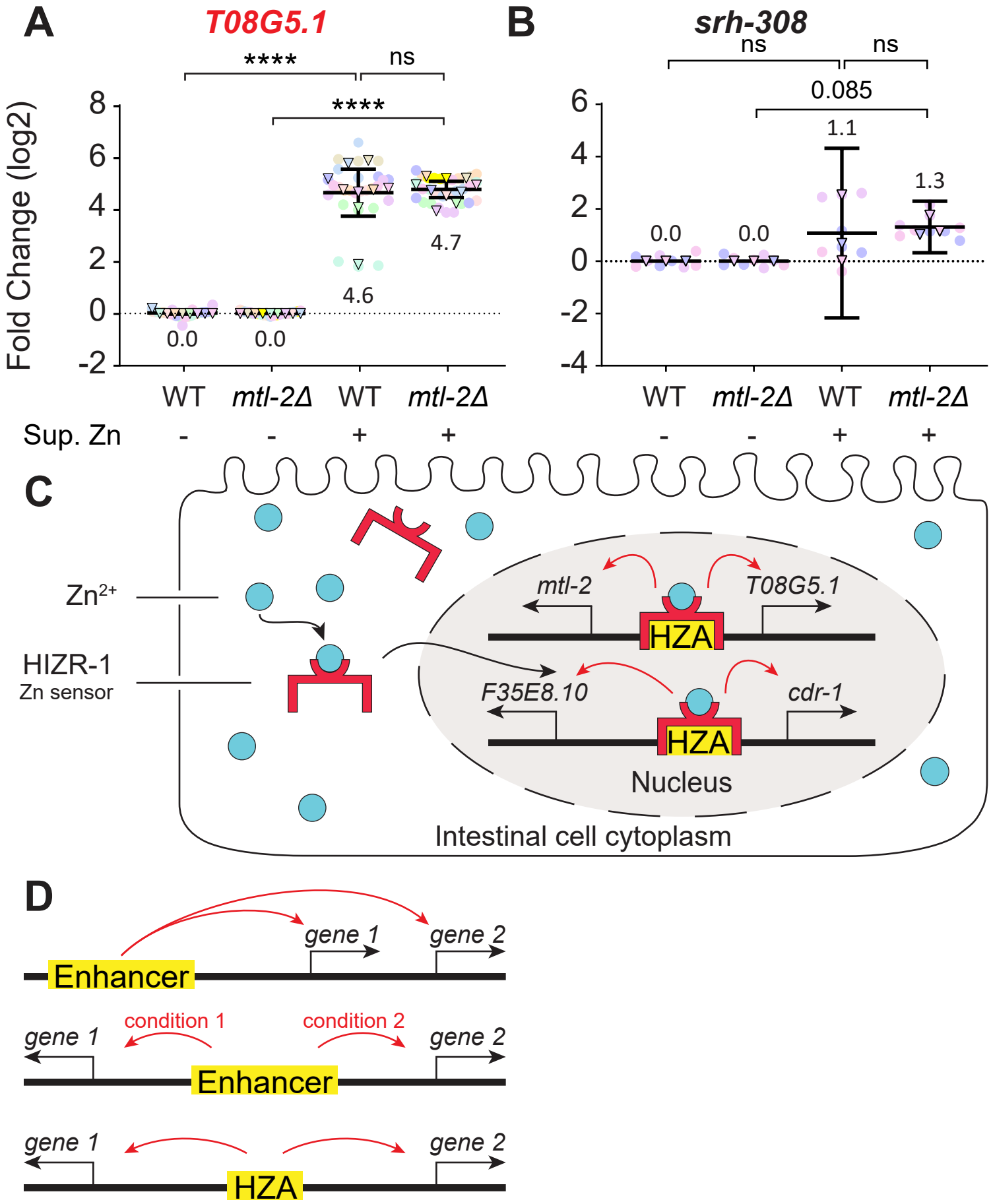
A
T08G5.1
****
ns
****
Fold Change (log2)
8
6
4
2
0
-2
0.0
0.0
4.6
4.7
WT
mtl-2Δ
WT
mtl-2Δ
Sup. Zn
-
-
+
+
B
srh-308
ns
ns
0.085
6
4
2
0
-2
-4
0.0
0.0
1.1
1.3
WT
mtl-2Δ
WT
mtl-2Δ
-
-
+
+
C
Zn2+
HIZR-1
Zn sensor
mtl-2
T08G5.1
HZA
F35E8.10
cdr-1
HZA
Nucleus
Intestinal cell cytoplasm
D
gene 1
gene 2
Enhancer
condition 1
condition 2
gene 1
gene 2
Enhancer
gene 1
gene 2
HZA

Figure 1. Two regions of Chromosome V have genes that are oriented head-to-head, induced by cadmium, and require *hizr-1*. **A, E)** Schematics of regions of Chromosome V are drawn to scale in base pairs (bp). Numeric chromosome location indicates the first base pair of the HZA. Thick black line represents DNA; yellow box indicates HZA enhancer; numbers are intervals from HZA enhancer to ATG initiation codon and end of transcript; arrows above represent pre-mRNA for indicated genes. Scale bar as shown. **D, H)** Distances from the HZA to the start codons (shown in panels A and E) plotted against fold change for WT plus cadmium (shown in B, C, F, and G). **B, C, F, G)** Wild type (WT) and *hizr-1(am286)* mutants at the L4 stage were cultured with or without 100µM cadmium for 16 hours and analyzed by qPCR. Values for WT and *hizr-1(am286)* with no cadmium were set equal to 0, and values with cadmium represent log2 fold change. N = 4 initial biological replicates, but may vary in panels due to outlier removal. Circles are technical replicates (repeated measurements of the same sample), and triangles are biological replicates (different samples from different days). Same color denotes the same experiment trial. Statistical analysis by pairwise one-way ANOVA. Non-significant p-values are listed for $p<0.3$; otherwise, "ns". For significant p-values: *<0.05; **<0.01; ***<0.001; ****<0.0001. Error bars represent mean ± 95% confidence intervals. Mean values are listed. All fold changes are in base 2 logarithm (e.g. 3 fold = 8x). The same approach is used to represent qPCR data in Figures 2-4. **Methods:** To age-synchronize the animals, we grew each strain on 90mm NGM dishes until the population was recently starved and most animals were adult stage. We washed the animals off the NGM dishes with M9 buffer into a 14ml falcon tube (M9 buffer: 1ml 1M $MgSO_4$, 3g KH_2PO_4, 6g Na_2HPO_4, 5g NaCl in 1L MilliQ (Stiernagle 2006)). We centrifuged and washed the worms with M9 buffer three times before one final centrifugation for a pellet. We added 5ml bleaching solution to the pellet and vortexed for three minutes to release

24 the eggs (bleaching solution: MilliQ, commercial Clorox bleach, and 1M NaOH at a ratio of
25 7:2:1). If live worms were still present, we extended vortexing for another 15 seconds. We
26 washed the eggs with M9 buffer twice and hatched them on 90mm unseeded NGM dishes. After
27 24 hours, we transferred the hatched L1 larvae onto 90mm seeded NGM dishes and cultured for
28 28 to 32 hours until most animals were L4 stage. To avoid crowding, which may reduce the
29 growth rate, we sometimes used two dishes. L4 animals were separated onto NAMM dishes
30 corresponding to different metal conditions. After 16 hours, we collected the animals for RNA
31 extraction according to previous publications (Warnhoff et al. 2017; Earley et al. 2021). Briefly,
32 we washed animals from NAMM dishes to an Eppendorf tube, pelleted to 100µl, and added
33 400µl TRIzol (Invitrogen Cat# 15596018). We subjected the tube to a liquid nitrogen-37°C
34 heatblock freeze cycle three times, added an additional 200µl TRIzol and 140µl chloroform
35 (Sigma-Aldrich Cat#319988), vortexed, and centrifuged. We purified the top aqueous phase
36 containing crude RNA extract using Qiagen RNeasy Mini Kit (Cat# 74106). For cDNA
37 synthesis, we used 1µg RNA and followed instruction from Intact Genomics igScript First Strand
38 cDNA Synthesis Kit (Cat# 4314) or BioRad iScript reverse transcription supermix for RT-qPCR
39 (Cat# 1708841). We substituted the water with Ambion nuclease-free water (Invitrogen Cat#
40 AM9937). We performed qPCR using MicroAmp fast optical 96-well reaction plate
41 (ThermoFisher Cat# 4346906) and BioRad iTaq Universal SYBR Green Supermix (Cat#
42 1725121) in an Applied Biosystems StepOne Plus thermocycler. The thermocycling program was
43 95°C for 20 seconds, then 40 cycles of 95°C for 3 seconds, and 60°C for 30 seconds. Primers for
44 qPCR were designed with the IDT PrimerQuest Tool (www.idtdna.com/PrimerQuest). The
45 primers are listed in Supplementary Table 2. For each biological replicate, we measured three
46 technical replicates for each gene (three wells). The results were collected as C_T cycles and

analyzed with $2^{-\Delta\Delta C_T}$ method in Microsoft Excel (Schmittgen and Livak 2008). GraphPad Prism 9 was used for statistical analysis and graphing. We first transformed the $2^{-\Delta\Delta C_T}$ values of each technical replicate by base 2 logarithm for normal distribution, and then removed outliers with ROUT method (Q=0.5%). We calculated the biological replicate data points as averages of the respective outlier-removed technical replicates. We analyzed the biological data with ANOVA or mixed-effects analysis with Holm-Šídák correction. Changes in expression levels of any given gene are reported as the average of all biological data in fold change; “3 fold” means 2^3, or “8 times”. We overlaid both technical and biological data into a single SuperPlot in Adobe Illustrator (Lord et al. 2020).

57 **Figure 2.** The HZA^{mT} element is necessary for zinc-induced transcription of both *mtl-2* and
58 *T08G5.1*. **A)** Schematic of a region of Chromosome V drawn to scale in base pairs (bp). Thick
59 black line represents DNA; yellow box indicates HZA enhancer. Arrows above represent
60 pre-mRNA for indicated genes. Red lines below indicate mutations: *gk125*, a deletion of the
61 *mtl-2* open reading frame; *syb4265*, a 15-bp deletion of the HZA^{mT} (named HZA$^{mT}\Delta$ below and
62 subsequent figures). Scale bar: 200bp. **B)** Alignment of the HZA^{mT} elements and their flanking 6
63 bp in different *Caenorhabditis* species and the *syb4265* deletion strain. **C-E)** Wild type (WT) and
64 *syb4265* mutants at the L4 stage were cultured with replete (-) or 200µM supplemental zinc (+)
65 for 16 hours and analyzed by qPCR. N = 15 initial biological replicates, but may vary in panels
66 due to outlier removal.

67 **Figure 3** The HZA^{cF} element is necessary for zinc-induced transcription of both *F35E8.10* and
68 *cdr-1*. **A)** Schematic of a region of Chromosome V drawn to scale in base pairs (bp). Thick black
69 line represents DNA; yellow box indicates HZA enhancer. Arrows above represent pre-mRNA
70 for indicated genes. Red line below indicates the *syb4134* mutation, a 14-bp deletion of the
71 HZA^{cF} enhancer (named HZA^{cF}Δ below and subsequent figures). Scale bar: 200bp. **B)** DNA
72 sequence of the HZA^{cF} element and flanking 6 bp in WT and *syb4134* mutant. **C-E)** Wild type
73 (WT) and *syb4134* mutants at the L4 stage were cultured with replete (-) or 200µM supplemental
74 zinc (+) for 16 hours and analyzed by qPCR. N = 15 initial biological replicates, but may vary in
75 panels due to outlier removal.

76 **Figure 4.** A deletion of *mtl-2* did not influence zinc-activated transcription of *T08G5.1*.
77 **A, B)** Wild type (WT) and *mtl-2(gk125)* mutants (shown in Figure 2 and denoted as *mtl-2Δ*) at
78 the L4 stage were cultured with or without 200μM zinc for 16 hours and analyzed by qPCR.
79 Biological replicates: *T08G5.1* N = 10, *srh-308* N = 3. **C)** Model for the orientation-independent
80 enhancer function of the HZA element. Within the intestinal cell, HIZR-1 (red) binds to zinc ions
81 (cyan circles) during zinc excess conditions and enters the nucleus. HIZR-1 binds the HZA
82 element (yellow) and upregulates both flanking genes in a head-to-head configuration. Black
83 arrows indicate movements, and red arrows indicate positive transcriptional regulation. Thick
84 black lines in the nucleus represent chromosome V, with arrows indicating transcription start
85 sites of genes. Figure not drawn to scale. **D)** Different mode of enhancer function. Top, a single
86 enhancer controls multiple genes encoded on the same DNA strand. Middle, a single enhancer
87 controls multiple genes encoded on different DNA strands under different conditions. Bottom,
88 the HZA enhancer controls head-to-head genes simultaneously under the same condition.